International Journal of Mass Spectrometry 300 (2011) 173–181

Contents lists available at ScienceDirect

International Journal of Mass Spectrometry

journal homepage: www.elsevier.com/locate/ijms

Solvent vapor effects on planar high-field asymmetric waveform ion mobility spectrometry

Leonard C. Rorrer III, Richard A. Yost*

Department of Chemistry, University of Florida, PO Box 117200, Gainesville, FL 32611-7200, United States

ARTICLE INFO

Article history:
Received 21 January 2010
Received in revised form 8 April 2010
Accepted 8 April 2010
Available online 23 April 2010

Keywords:
FAIMS
Solvent vapor effects
Explosives
Mass spectrometry
Electrospray

ABSTRACT

The effects of various concentrations of solvent vapor (either water or methanol) added to the curtain/drift gas in a planar high-field asymmetric waveform ion mobility spectrometer (FAIMS) have been examined. Two different groups of analyte ions (the $[M-H]^-$ ions of three positional isomers of phthalic acid and the M^- and $[M-H]^-$ ions of four explosives: TNT, 2,4 DNT, 2,6 DNT, and 3,4 DNT) were analyzed. Results showed that with the addition of small amounts of solvent vapor (~1.5% water and 12.3% methanol), there were dramatic shifts to larger CV values for all ions analyzed. There were substantial benefits provided by adding solvent vapor, including dramatically increased resolving power of isomeric ions (up to ~141). Specifically, analyte ions examined in dried nitrogen exhibited overlapping, undistinguishable CV values, but with large CV shifts afforded by addition of solvent vapor, these analyte ions were completely resolved from one another.

1. Introduction

High-field asymmetric waveform ion mobility spectrometry (FAIMS) separates and filters ions generated by various atmospheric pressure ionization methods [1,2]. FAIMS is similar to conventional ion mobility spectrometry (IMS) in that it uses the motion of ions produced by an applied electric field to achieve separation. Further, this ion motion occurs in a drift gas, typically at one atmosphere. The major difference between the two techniques is the magnitude of and method of applying the electric field. In conventional IMS, a low constant electric field, generally less than 200 V/cm, is applied parallel to the direction of separation, and is used to move the ions through the drift gas inside the spectrometer. In FAIMS, a much higher electric field, generally greater than 10,000 V/cm, is applied perpendicular to the direction of separation and the drift gas is used to move the ions in the direction of separation. The electric field in FAIMS is also not constant, with an asymmetric waveform alternating between periods of opposite-polarity.

The principles of operation of FAIMS were first described by Buryakov et al. [3] and further detailed by Guevremont et al. [1,2,4] Ions that are subjected to an electric field in a drift gas will move along the applied field lines with a velocity given by Eq. (1),

$$v = K \times E \tag{1}$$

where v is the drift velocity of the ion, K is the coefficient of ion mobility, and E is the applied electric field strength. At low electric fields, ~200 V/cm, K is independent of applied electric field and ions with different K values travel at different velocities [3,5]. Conventional IMS uses these velocities to achieve separation.

At the higher electric fields used in FAIMS, >~10,000 V/cm, K becomes dependent on applied field strength in a non-linear manner [3]. The high-field mobility is referred to K_h, a high-field mobility term, that varies depending on field strength. The dependence of mobility at high-field can be described by Eq. (2),

$$K_h = K\left[1 + \alpha\left[\frac{E}{N}\right]^2 + \beta\left[\frac{E}{N}\right]^4 \cdots\right] \tag{2}$$

where K_h is the high-field mobility, K is the low-field mobility, E is the applied electric field in V/cm, N is the gas number density in molecules/cm^3, and α and β are ion-specific dependencies on applied electric field (i.e., the $[M+H]^+$ and M^+ ions may have different α and β) [4].

To generate the high fields used in FAIMS, typically a radio frequency (RF) asymmetric waveform is applied to one plate while the other plate is held at or near ground. This asymmetric waveform, $V(t)$, is composed of a high-voltage portion, often referred to as dispersion voltage (DV, 0 to peak) applied for a short period of time (V_1 and t_1) and a lower voltage, opposite-polarity portion applied for a longer period of time (V_2 and t_2). The sum of the time–voltage

---

* Corresponding author. Tel.: +1 352 392 0557; fax: +1 352 392 4651.
E-mail address: ryost@chem.ufl.edu (R.A. Yost).

1387-3806/$ – see front matter © 2010 Elsevier B.V. All rights reserved.
doi:10.1016/j.ijms.2010.04.002

products of the waveform is equal to zero, as shown in Eq. (3) [2–4],

$$V_1 \times t_1 + V_2 \times t_2 = 0 \tag{3}$$

As a result of the high-field dependence on ion mobility, ions will experience two different mobilities during one cycle of the asymmetric RF waveform, which generates two different velocities (Eq. (1)). As ions are moved pneumatically through the cell perpendicular to the applied field, they will experience a net displacement towards one of the electrodes if there is a sufficient difference between the two velocities. If an ion experiences enough cycles of the asymmetric waveform, it will strike one of the two electrodes and be neutralized. To offset an ion's net displacement, a small direct current (DC) potential is applied to one of the electrodes and is referred to as a compensation voltage (CV). This CV value is essentially a measure of the difference in mobility of an ion at the two different applied fields. Since K_h is ion-dependent, the magnitude of the CV needed to offset the net displacement will be different for different ions, including isomeric ions [6–8]. Under the conditions appropriate to transmit one ion, i.e. correct DV and CV, other ions will drift towards one of the plates and be lost. FAIMS spectrometers essentially act as ion filters which selectively transmit ions with the appropriate ratio of K_h to K. A mixture of compounds can be analyzed by scanning the CV over a range of voltages, producing a CV spectrum. The CV can also be held constant, allowing specific ions to be transmitted [1,3,4].

In general, FAIMS spectrometers are composed of two plates, planar or curved, placed a uniform distance apart. Planar geometries typically offer higher specificity and resolving power at a cost of lower transmission [9], whereas curved geometries offer greater transmission due to an electrostatic focusing effect at a cost of lower resolving power [10,11]. Resolving power for a FAIMS spectrometer is defined by Eq. (4),

$$R_p = \frac{|\mathrm{CV}|}{\mathrm{RWHM}} \tag{4}$$

where R_p is the resolving power, $|\mathrm{CV}|$ is the absolute value of the measured compensation voltage for a particular ion, and FWHM is the full width in volts at half maximum height for the CV peak. Resolving power is an instrumental parameter that estimates how well the instrument (and conditions under which it is operating) can separate or resolve two ions with similar behaviors [12,13]. The resolution between two neighboring peaks is defined by Eq. (5),

$$R_S = \frac{|\mathrm{CV}_2 - \mathrm{CV}_1| \times 2}{\left[\mathrm{PW}_{2_{10\%}} + \mathrm{PW}_{1_{10\%}}\right]} \tag{5}$$

where R_s is the resolution, CV_1 and CV_2 are the CV values for the ions of interest, and $\mathrm{PW}_{1_{10\%}}$ and $\mathrm{PW}_{2_{10\%}}$ are the peak widths in volts at 10% of the full height.

As shown in Eq. (2) above, the dependence of K_h on high-field depends on two ion-specific terms, α and β. The reasons why different ions have different α and β terms are not fully understood. Of particular interest to us is how ion chemistry can affect those terms, and therefore the way ions behave in the FAIMS spectrometer. Previous work has shown that when water vapor concentrations or contamination in the drift gas is high, there are very apparent chemical effects [4,14–17]. When water or other vapors are present in the carrier gas, an ion may collide with those neutral molecules and form complexes. These complexes in turn may have different mobilities at the two different fields used in FAIMS as compared to the bare ion. In FAIMS spectrometers using curved plates, these complexed ions will not be efficiently resolved, or may be lost all together from the FAIMS spectrometer due to the focusing effect [1,4,10,11]. Indeed, it is critical that dry gases be used with curved plate geometry. Otherwise, ion CV peaks broaden and signal is lost altogether [2,14]. Due to this demand for dry gas in curved plate FAIMS spectrometers, it has been shown that careful selection of ionization and injection conditions at the entrance of the FAIMS spectrometer is important for good performance. Particularly important are the flow rate of the solution into the ionization source, the flow rate of the drift gas and the solvent composition of the analyte solution [14].

Eiceman and coworkers showed that concentrations of water in the drift gas above approximately 50 ppm caused CV shifts of organophosphorus ions using a micromachined planar FAIMS spectrometer [16]. These shifts were explained by a formation of water-ion complexes during the lower voltage portion of the asymmetric waveform which were dissociated to bare ions during the higher voltage portion of the waveform. The complexation of the ions was enough to change their mobility so that the difference between the lower field mobility and higher field mobility changed [15,18]. This group also reported the addition of dopant compounds to the carrier gas to assist in the detection of explosives [17]. Other groups have shown separation of the isomers of phthalic acid by the addition of carbon dioxide to the carrier gas [7,19].

Much of the work exploring the effects of solvent vapors or contaminants has concentrated on either curved FAIMS spectrometers coupled with mass spectrometry or micromachined planar FAIMS spectrometers. Both of these geometries offer some interesting insights into the effects of solvent vapor on performance of the FAIMS spectrometer. For curved geometries, detailed investigations into solvent vapor effects using high concentrations are not possible, as the focusing effect causes a dramatic decrease in ion signal or a complete loss of ion signal all together [4,14,15]. The main focus for research on the effects of solvent vapor in curved geometry has therefore been how to limit and control the levels of vapors allowed to enter the spectrometer. Ion signal in a micromachined planar geometry FAIMS spectrometer is not as affected by solvent vapor due to the lack of ion focusing effect. Micromachined geometries, however, do not offer very high resolving powers due to the small size and short ion residence time. It has been shown that the resolving power of a FAIMS spectrometer, particularly planar geometries, increases as the residence time inside the cell increases [20,21]. Higher resolving power planar FAIMS spectrometers have been built by Smith and coworkers, showing resolving powers up to at least 40 [21]. The use of such high resolving power FAIMS spectrometers to monitor the effects on performance with the addition of solvent vapor can provide some additional insight into the how and why solvent vapor affects ions as they move through the FAIMS cell.

This study focuses on using a high resolving power planar FAIMS spectrometer to monitor the effects on ions when solvent vapors are added to the cell in controlled amounts. Ions generated by either electrospray ionization (ESI) or atmospheric pressure chemical ionization (APCI) were analyzed and the CV value, peak width and ion signal were monitored as the concentration of solvent vapor (methanol or water) was changed. The effect on CV value, peak width, and ion signal as a function of solvent vapor concentration can lead to a better understanding of the ion chemistry inside the FAIMS spectrometer. The use of a high resolving power FAIMS spectrometer provides a greater opportunity to monitor small changes in CV peaks to help elucidate the progression of solvent effects. The analytical potential and practicality of addition of solvent vapor to the carrier gas have also been investigated.

2. Experimental

2.1. Instrumentation

All of the work reported herein was performed using a custom built planar FAIMS spectrometer. The FAIMS cell consisted of two

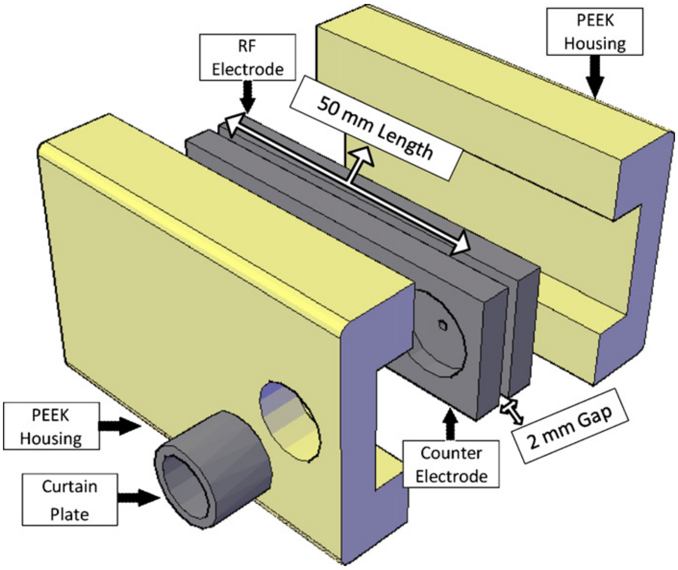

Fig. 1. Custom built planar FAIMS spectrometer.

polished parallel plates 20 mm × 65 mm in overall size housed in a plastic (PEEK) enclosure (Fig. 1). The parallel plates were held a uniform distance apart to create the analytical gap through which the carrier gas moved the ions. This gap was 2.0 mm for all of the experiments described. The cell was constructed such that ions could be injected into the cell either parallel or orthogonal to the direction of ion separation. All of the work described here used orthogonal injection giving, an effective cell length of 50 mm. Ions first pass through a curtain plate/curtain gas interface before entering into the FAIMS cell. The gas (nitrogen) was introduced to the FAIMS spectrometer in the region between the curtain plate and the entrance into the cell. A portion of this gas is drawn into the cell and serves as the FAIMS drift gas, while the bulk of the gas exits through the curtain plate/curtain gas interface and aids in the desolvation of the ions. The asymmetric waveforms and compensation voltage (CV) were generated using a Thermo Scientific FAIMS waveform generator (San Jose, CA) operating at 750 kHz. For all of the studies, the dispersion voltage (DV) was kept constant at $-3500\,V_{0\text{-}p}$ and the CV was scanned over the range of interest. Ions were mass analyzed after passing through the FAIMS spectrometer using a Finnigan TSQ7000 triple quadrupole mass spectrometer (San Jose, CA). The exit of the FAIMS spectrometer was interfaced directly to the heated capillary interface of the mass spectrometer. This interface was sealed such that the carrier gas flow rate through the FAIMS cell was controlled by the flow rate into the mass spectrometer. This flow rate was approximately 0.7 L/min for all of the experiments described below. Ions were generated using either a custom electrospray ionization (ESI) source or a modified TSQ7000 atmospheric pressure chemical ionization (APCI) source, depending on the type of analyte. Ionization conditions were monitored and set to provide the highest ion signal for each set of analytes.

2.2. Materials

Two different sets of analytes were studied. The three positional isomers of phthalic acid were studied, as previous work has shown that the isomers exhibit different behaviors in FAIMS experiments and can be separated [7,22]. The identity of the isomer cannot be determined using mass spectrometry alone or using conventional IMS [23]. Four explosives, trinitrotoluene (TNT) and three positional isomers of dinitrotoluene (2,4, 2,6, and 3,4) were also studied. Previous work has shown that the FAIMS can provide high levels of sensitivity and selectivity for the detection of explosives [17,24]. The solvents used in these studies, HPLC grade water and methanol, were obtained from Fisher Scientific (Waltham, MA). The *o*-, *m*-, and *p*-isomers of phthalic acid were obtained from Acros Organics (Geel, Belguim). The phthalic acid isomers were dissolved and diluted to a final concentration of 50 ppm each in 90%/10% methanol/water with 0.2 mM ammonium acetate. The individual isomer solutions were ionized by negative ESI, producing $[M-H]^-$ ions. The four explosive samples were provided by the Analytical Laboratory of Israeli Police Headquarters. The individual explosive analytes were diluted to a final concentration of 20 ppm each in 65%/35% methanol/water and ionized using negative APCI, producing M^- and $[M-H]^-$ ions. Nitrogen was used as both the curtain and carrier gas for all experiments. The nitrogen was obtained from boil-off from a liquid nitrogen dewar and was then passed through a hydrocarbon/moisture trap (Agilent, Santa Clara, CA) to remove any impurities and dry the gas.

2.3. Procedures

Each analyte was analyzed individually using either dried nitrogen or dried nitrogen with various concentrations of solvent vapor (water or methanol), added to the curtain/drift gas. To obtain the various concentrations of solvent vapor, dried nitrogen was sparged through a volume of the solvent of interest in a sealed bottle kept at room temperature (~22 °C). The headspace of this bottle was then taken and mixed with additional dried nitrogen to obtain the final desired concentration. The amount of solvent present in the gas was measured by determining the amount of weight lost after set amounts of gas were passed through the solvent. The setup used here provided solvent-saturated gas at the flow rates used in the studies (3.5–3000 mL/min). The maximum concentration for water was 17,500 ppm (w/v) and 123,000 ppm (w/v) for methanol. For each experimental condition, the CV was scanned over the range of interest producing a CV spectrum. The mass spectrometer was set to acquire data in selected ion monitoring mode for the ions of interest. The changes in CV value at the centroid of the analyte peak, peak width at FWHM, and the ion signal intensity were monitored to determine the effects of solvent vapor on behavior in the FAIMS spectrometer.

3. Results and discussion

3.1. Concentration effects

3.1.1. Phthalic acid isomers

Fig. 2a–c shows plots of the CV value, FWHM, and normalized signal intensity (normalized to value in dried nitrogen) for the $[M-H]^-$ ions of the three isomers of phthalic acid as a function of water vapor concentration in the nitrogen curtain/drift gas. Fig. 3a–c shows the same plots for the three phthalic acid isomers versus concentration of methanol vapor. The three isomers showed different CVs, peak widths and intensities as the concentration of water or methanol increased. It is not known if the decrease in signal for all three isomers is a function of the presence of solvent vapor inside the FAIMS spectrometer or due to the effect of curtain gas containing solvent vapor on the electrospray ionization process. The ESI configuration used in these experiments did not use a sheath gas to aid in desolvation of the ions, so the presence of solvent in the curtain gas, which is used to aid desolvation, may have affected the intensities of the $[M-H]^-$ ions.

The $[M-H]^-$ ions of the *m*- and *p*-isomers showed some similar behavior, especially in the changes in FWHM at lower concentrations and CV shift. For all three isomers, there was initially peak broadening at low concentrations. As the concentrations increased,

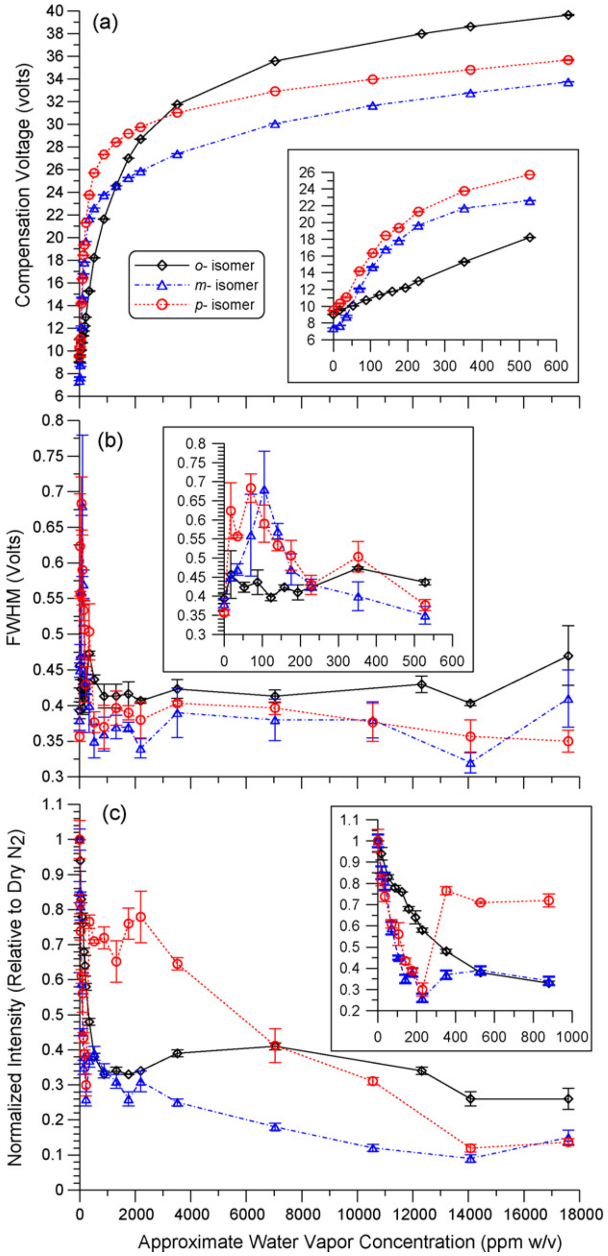

Fig. 2. Plots of CV value (a), FWHM (b), and normalized signal intensity (c) for the [M−H]⁻ ions of the *o*- (D), *m*- (C), and *p*- (A) isomers of phthalic acid with various concentrations of water vapor added to the nitrogen curtain/carrier gas. The insets in the figures expand the regions at lower concentrations.

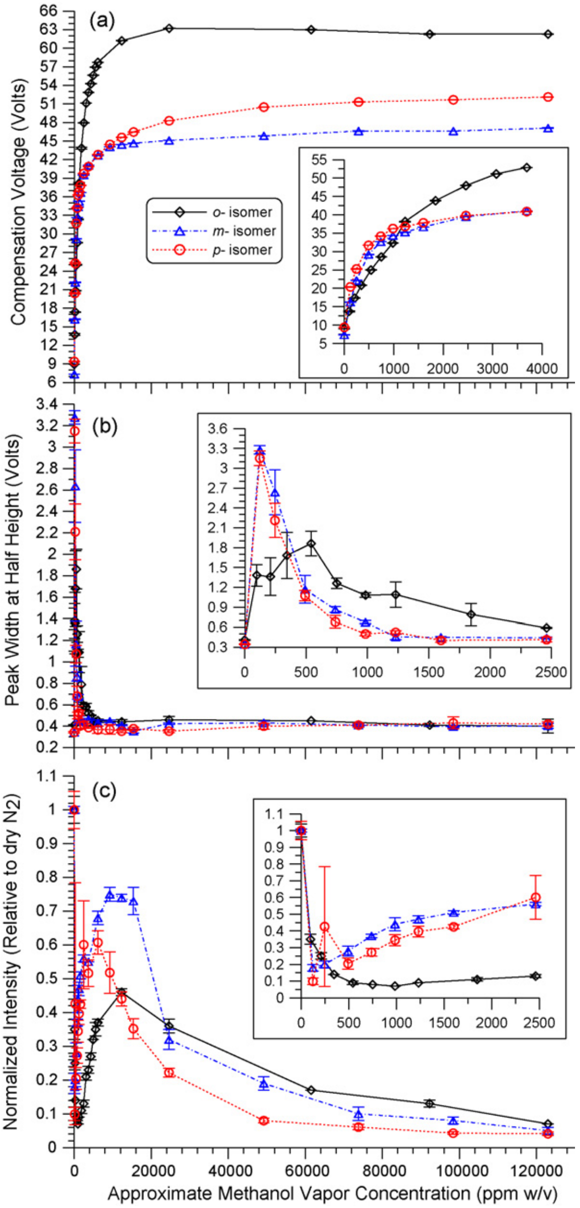

Fig. 3. Plots of CV value (a), FWHM (b), and normalized signal intensity (c) for the [M−H]⁻ ions of the *o*- (◊), *m*- (△), and *p*- (○) isomers of phthalic acid with various concentrations of methanol vapor added to the nitrogen curtain/carrier gas. The insets in the figures expand the regions at lower concentrations.

the peak widths returned to approximately the value measured in dried nitrogen. The CV values for the isomers all increased with increasing concentration, before beginning to level off at the highest concentrations achievable. The concentration levels at which peak widths return to approximately the original values and CV values begin to level off are similar.

The observations made here are most likely due to clustering interactions between the ions and solvent vapor inside the cell. Eiceman et al. stated that concentrations of vapors or contaminants above approximately 50 ppm can affect the performance of the FAIMS spectrometer [15]. As ions are moved through the FAIMS spectrometer by the drift gas, they are being oscillated in opposite directions by the asymmetric RF waveform. The oscillation imparts kinetic energy or “heats” the ions, and asymmetry in the waveform causes the ions to experience two different ion temperatures. During the high-field portion of the waveform, the ions will be “hotter”, increasing the likelihood that they will be unsolvated or unclustered “bare” ions. During the low-field portion of the waveform, the ions will be “cooler”, and more likely to be solvated or clustered with solvent molecules forming clustered ion-neutral species. These clustered species will tend to have lower mobilities in the drift gas, as they are larger than the unclustered species. This decrease in mobility will increase the net difference between the high-field and low-field mobilities. As mentioned above, the CV is used to offset net displacements inside the cell caused by differences in high- and low-field mobility. The increase in the mobility difference means that additional voltage will be needed to compensate for the amount of net displacement inside the FAIMS spectrometer, increasing the CV.

The observation of initial peak broadening and then narrowing supports the theory of clustering of solvent molecules around the ions and suggests a possible mechanism. As solvent vapor is first

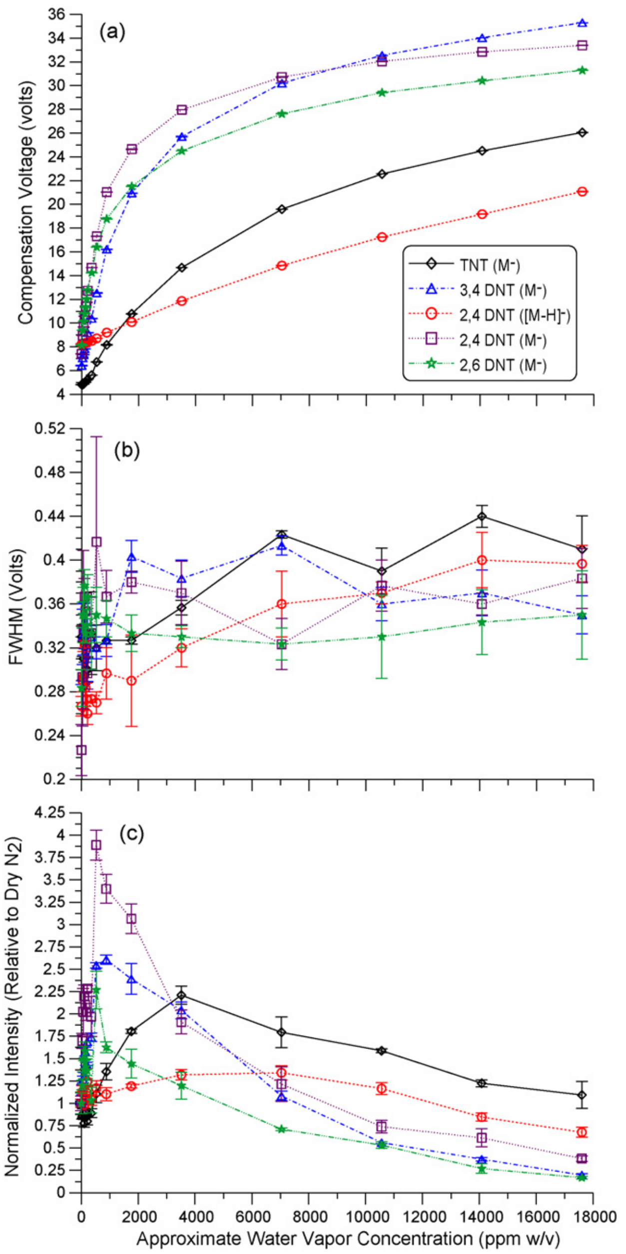

Fig. 4. Plots of CV value (a), FWHM (b), and normalized signal intensity (c) for the M^- ions of TNT (◊), 3,4 DNT (△), 2,4 DNT (◯), and 2,6 DNT (□) and the $[M-H]^-$ ion of 2,4 DNT (⋆) with various concentrations of water vapor added to the dried nitrogen curtain/carrier gas.

introduced into the FAIMS spectrometer and the concentrations are low, some ions may have more solvent molecules attached than other ions. This creates a broad distribution in the extent of solvation. This distribution also creates a distribution in the mobilities during the low-field portions of the waveform and therefore a distribution in net displacements for the ions of interest. This range of net displacements requires a broad range of CV values to transmit ions effectively and creates a broad peak.

As more solvent is added, the ion-solvent clusters begin to all approach a maximum size and no more solvent molecules can be added [25–27]. This “complete” solvation at low-field means all ions no longer exhibit a distribution of mobilities but have a single low-field mobility. At this stage there should be a single net displacement, as there is only one low-field mobility and one high-field mobility. The peak width returning to approximately the value in dried nitrogen at these higher concentrations adds support for this theory. Presumably in dried nitrogen, ions would exist with two distinct mobilities as there would be no solvent vapor present to create clusters. Other support for this theory is seen in the plots of CV value. As mentioned above, the clustering of solvent with the ions at low-field leads to the increase in CV value. If the ions reach a state of “complete” solvation at low-field, the CV value should reach a maximum. As the concentration of solvent vapor increases, there is an initial large increase in CV value. At higher solvent vapor concentrations, the CV values begin to level off, reaching a maximum signifies that ions are nearing “complete” solvation at low-field.

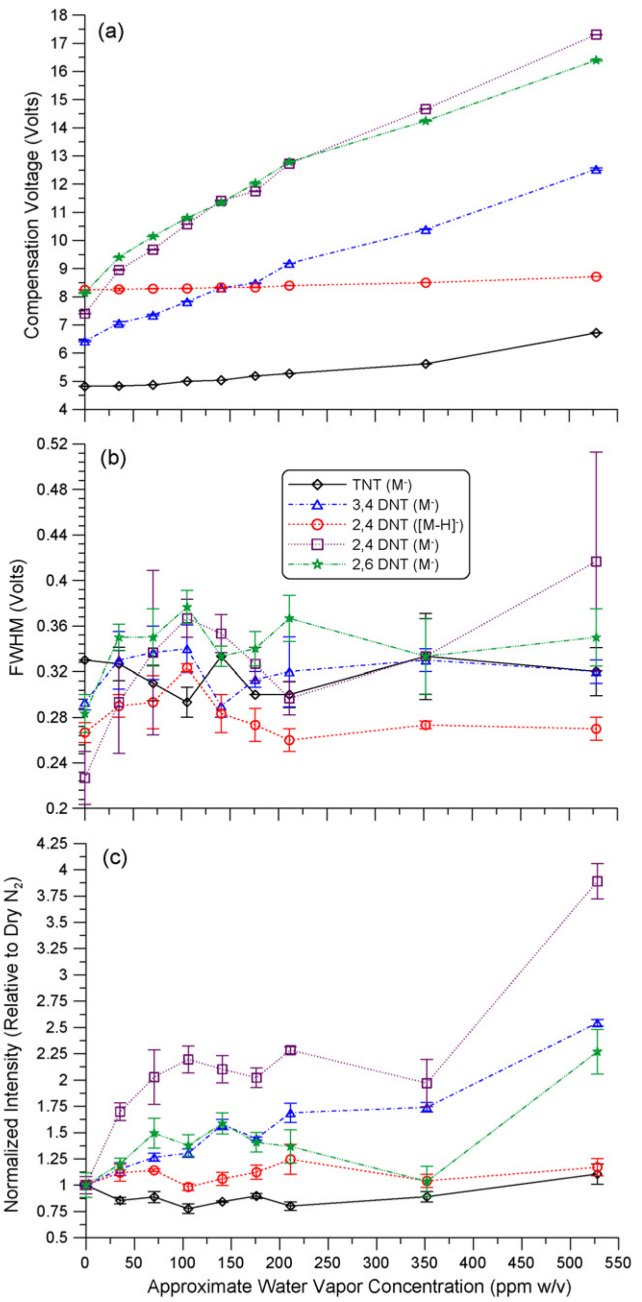

Fig. 5. Zoomed-in plots of CV value (a), FWHM (b), and normalized signal intensity (c) for the M^- ions of TNT (◊), 3,4 DNT (△), 2,4 DNT (◯), and 2,6 DNT (□) and the $[M-H]^-$ ion of 2,4 DNT (⋆) with various concentrations of water vapor added to the dried nitrogen curtain/carrier gas.

The plot for the CV value for *o*-phthalic acid with methanol vapor concentration also showed a slight decrease in CV value at the highest concentrations achievable. One possible cause of this is that at the high concentrations present, not only is the low-field ion “completely” solvated, some of the high-field ions start to become solvated. This would decrease the net displacement in the FAIMS spectrometer lowering the CV value needed to transmit the ions. Note that no peak broadening was observed at high methanol concentrations. The phthalic acid isomers’ behavior shown here has some correlation to the previously published work showing the effects on the isomer ions behavior with the addition of carbon dioxide to the drift gas [7]. Particularly, similar effects were observed in the increase in the CV value as the concentration of carbon dioxide increased and the similar behavior of the *m*- and *p*-isomers.

3.1.2. Explosives

Fig. 4a–c shows the plots of CV value, FWHM, and normalized signal intensity (relative to value in dried nitrogen) for four explosives as a function of the water vapor concentration in the nitrogen curtain/drift. Fig. 5 shows zoomed-in plots for the regions at low concentrations for Fig. 4. The M^- ions of the four explosives showed similar trends in CV value as were observed for the $[M-H]^-$ ions of the isomers of phthalic acid. There was a large increase in CV value as the concentrations of water vapor increased before beginning to level off and approaching a maximum at the highest vapor concentrations achievable.

Differences in the behavior of the explosive analytes and phthalic acid isomers were observed in which ionic species reacted. Negative APCI of the explosive analytes produced the M^- ion as the major ion for TNT, 3,4 DNT and 2,6 DNT, with an $[M-H]^-$ ion at 0.25–2% relative abundance. In contrast, APCI of 2,4 DNT generated both an M^- ion and an $[M-H]^-$ ion, with the latter being the 5–10 times more abundant. The behavior of the $[M-H]^-$ ion of 2,4 DNT was very different from the M^- ion. As the concentration of water vapor increased, there was a very gradual increase in CV for the $[M-H]^-$ ion as compared to the M^- ion. It was also observed that as the concentration of water vapor increased, there was an initial large increase in the signal intensity for the M^- ions before a decrease at higher concentrations. The $[M-H]^-$ ion had very little if any signal increase before decreasing at higher water vapor concentrations. The reasons for the changes in signal and sensitivity were not investigated.

The increases in the CV values of the ions is likely due to clustering of solvent molecules around the ions during the low-field portion of the asymmetric RF waveform, as was theorized for the phthalic acid isomers above. However, the lack of any significant peak broadening as was seen with the phthalic acid isomers, specifically the *m*- and *p*-isomer, may indicate differences in the way solvent molecules cluster around the ions. As mentioned above, peak broadening may be indicative of a broad distribution of solvation levels at low-field. To put it in general terms, some ions may have one solvent molecule attached whereas others may have two or more solvent molecules attached. For the explosive ions, there may be a much narrower distribution of solvation levels. This narrower distribution may in turn yield an ion with two “distinct” high and low-field mobilities, and thus the CV peak width would stay relatively unchanged.

Eq. (6) represents the formation equilibrium for a negative ion and a negative ion clustered with n solvent molecules with a formation constant of K_f. Differences in ion chemistry and clustering:

$$\text{ion}^- \xleftrightarrow{K_f} \text{ion}^{-\bullet}(\text{solvent})_n \qquad (6)$$

mechanisms will yield different K_f values for different compounds and even for different ionic species of individual compounds. Further experiments to help understand this formation equilibrium and potentially take advantage of the behaviors of ions with the addition of solvent vapor are important in the development of FAIMS as an analytical technique.

3.1.3. Increased resolution with solvent vapor

These experimental results suggest that there may be practical analytical benefits from solvent vapor in FAIMS. Looking at the graphs for the shift in CV with addition of solvent vapor, one can see that in dried nitrogen there is often overlap of analytes. As the solvent vapor concentrations increase, the individual analytes shift at different rates and generally move farther from one another. Note that a greater difference in CV values (the differences between the centroids of the peaks) does not guarantee improved resolution of A from peak B, since that is also affected by peak width. To clarify the effect of solvent vapor on resolution, the analytes were ana-

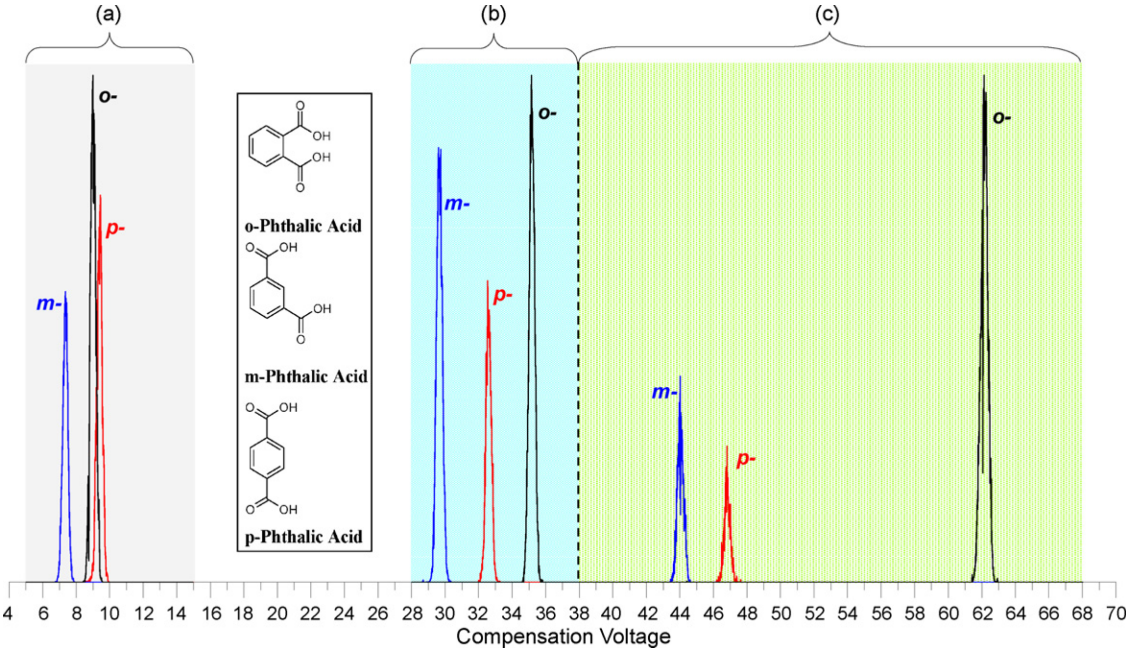

Fig. 6. CV scans of three phthalic acid isomer mixture acquired with different solvent vapor conditions. CV scan (a) was acquired in dry nitrogen. CV scan (b) was acquired with ~7000 ppm water vapor added to the dry nitrogen. CV scan (c) was acquired with ~15,000 ppm methanol vapor added.

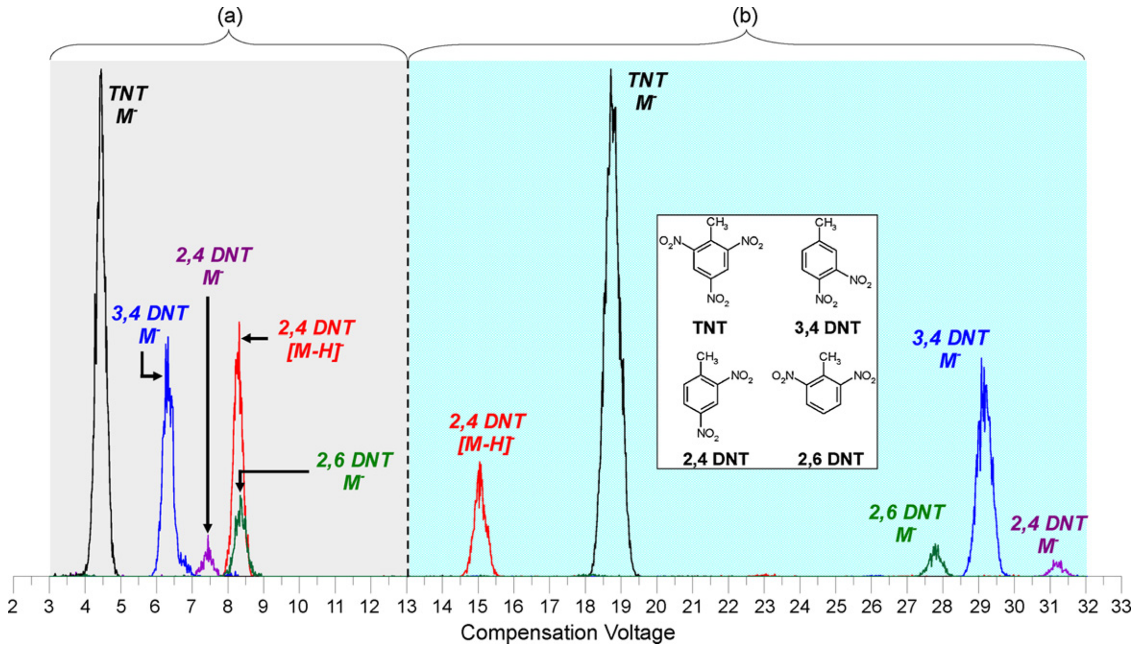

Fig. 7. CV scans of TNT and three DNT isomers (3,4, 2,4 (M⁻), 2,4 [M−H]⁻, and 2,6) acquired with different solvent vapor conditions. CV scan (a) was acquired in dry nitrogen. CV scan (b) was acquired with ~7000 ppm water vapor added.

lyzed in dried nitrogen and those results were compared to results obtained using a set concentration of solvent vapor added to the curtain/carrier gas. Concentrations were chosen by picking points on the graphs were the analytes showed significant differences in CV as well as reasonable signal intensities and peak widths that were approximately back to the values in dried nitrogen. The values used were ~7000 ppm (w/v) for water vapor and ~15,000 ppm (w/v) for methanol vapor.

Fig. 6a–c shows three CV spectra for the isomers of phthalic acid acquired under three different solvent conditions; dried nitrogen, water vapor added, and methanol vapor added, respectively. Traces for the [M−H]⁻ ion of individual analytes are shown to aid in distinguishing one compound from another however a mixture of analytes did exhibit the same overall CV spectrum. For dried nitrogen (Fig. 6a), the *m*-isomer was separated and baseline resolved from the *o*- and *p*-isomers. The *o*- and *p*-isomers showed some separation but were not resolved from one another, and in a mixture would appear as a single peak with two maxima. With the addition of ~7000 ppm water vapor, the [M−H]⁻ ions of the three isomers moved away from their dried nitrogen values by different amounts, significantly increasing their separation. The *o*-isomer moved much more than the other two isomers allowing all three isomers to be resolved. With the addition of ~15,000 ppm methanol vapor, the [M−H]⁻ ions of the three isomers moved even further from their initial positions in dried nitrogen, further increasing the resolution between the individual peaks. Table 1 summarizes the CV values, resolving power and resolution for the individual CV spectra. The data shown in the table are the averages from three scans plus/minus the standard error. The first column in each section lists the CV value at the centroid of each individual peak. The second column lists the resolving power at each peak, as calculated by Eq. (3). The third column lists the resolution between neighboring CV peaks, as calculated by Eq. (4). If two peaks have a resolution value above one, they are considered to be baseline resolved [12].

For the dried nitrogen case, all three phthalate ions exhibited different CV values. However, as is seen in Fig. 6a, the *o*- and *p*-isomers are not fully resolved, with a resolution value less than one (~0.67). The maximum resolving power for the FAIMS spectrometer is ~27. With the addition of ~7000 ppm water, the CV values for all three isomers increased. The order in which the isomers appeared in the spectrum also changed, as the *o*- and *p*-isomer switched positions. The calculated resolution between peaks also increased, with values now well above one. Maximum resolving power increased to ~89 due to an increase in CV value while maintaining relatively narrow peak widths. With the addition of ~15,000 ppm methanol vapor, there were further increases in CV values, although the order of the isomeric ions stayed the same as seen with water vapor added. The calculated resolution between peaks decreased slightly for the *m*- and *p*-isomers but was still well above the baseline resolution threshold of one. The calculated resolution between the *o*- and *p*-isomer increased dramatically over the value seen with water vapor added due to the very large increase in CV value for the *o*-isomer. The maximum resolving power for the FAIMS spectrometer

Table 1
Increased resolution of [M−H]⁻ ions of phthalic acid isomers with solvent vapor.

	Dried nitrogen				~7000 ppm water				~15,000 ppm methanol		
	CV	R_p	R_s		CV	R_p	R_s		CV	R_p	R_s
m-	7.37 ± 0.02 V	20.5 ± 0.5		*m*-	29.65 ± 0.02 V	71.7 ± 2.2		*m*-	43.79 ± 0.09 V	114.2 ± 4.8	
			2.42 ± 0.05				4.17 ± 0.05				3.4 ± 0.1
o-	8.99 ± 0.02 V	22.3 ± 0.5		*p*-	32.58 ± 0.03 V	88.9 ± 1.8		*p*-	46.53 ± 0.07 V	114.2 ± 5.2	
			0.67 ± 0.08				3.98 ± 0.04				18.3 ± 0.4
p-	9.45 ± 0.02 V	27.0 ± 0.3		*o*-	35.36 ± 0.03 V	86.1 ± 1.8		*o*-	62.18 ± 0.10 V	140.6 ± 3.5	

Table 2
Increased resolution of the M⁻ and [M−H]⁻ ions of four explosives.

	Dried nitrogen				~7000 ppm water		
	CV	R_p	R_s		CV	R_p	R_s
TNT (M^-)	4.46 ± 0.01 V	13.9 ± 0.4		2,4 DNT ($[M-H]^-$)	15.10 ± 0.02 V	40.4 ± 1.2	
			3.07 ± 0.03				4.6 ± 0.05
3,4 DNT (M^-)	6.29 ± 0.02 V	18.5 ± 0.3		TNT (M^-)	18.70 ± 0.03 V	37.6 ± 0.8	
			1.82 ± 0.06				11.34 ± 0.17
2,4 DNT (M^-)	7.40 ± 0.02 V	27.8 ± 1.8		2,6 DNT (M^-)	27.76 ± 0.02 V	78.8 ± 4.4	
			1.45 ± 0.03				1.88 ± 0.03
2,4 DNT ($[M-H]^-$)	8.25 ± 0.02 V	30.0 ± 1.6		3,4 DNT (M^-)	29.18 ± 0.01 V	69.7 ± 1.8	
			0.20 ± 0.04				2.7 ± 0.03
2,6 DNT (M^-)	8.37 ± 0.01 V	25.8 ± 0.6		2,4 DNT (M^-)	31.25 ± 0.01 V	81.8 ± 3.3	

was ~141, once again due to the large increase in CV value while maintaining relatively narrow peak widths.

Fig. 7a and b shows two CV spectra for four explosives acquired under different solvent conditions: dried nitrogen and ~7000 ppm water vapor added to the curtain/drift gas. Individual traces for the M^- ion of the four analytes (and for the $[M-H]^-$ ion of 2,4 DNT) are shown to aid in distinguishing one compound from another. For dried nitrogen (Fig. 7a), the M^- ions of TNT, 3,4 DNT and 2,4 DNT were separated from one another. The $[M-H]^-$ ion of 2,4 DNT, however, completely covered the peak for M^- ion of 2,6 DNT. This means that in a mixture, 2,6 DNT would not easily be detected without mass spectrometric assistance (i.e. the peaks are not separated in CV but the M^- ion of 2,6 DNT is m/z 182 and the $[M-H]^-$ of 2,4 DNT is m/z 181). With the addition of ~7000 ppm water vapor (Fig. 7b), however, all of the species in the dried nitrogen CV spectrum (Fig. 7a) shifted to new positions and were fully resolved from one another. The order of the ions also changed due to different levels of behavior with the addition of water vapor. Most interesting, as was seen in Fig. 4a, is the dramatic difference in CV shifts of the $[M-H]^-$ ion and M^- ion of 2,4 DNT. With addition of less than 1% water vapor to the carrier gas, these ions went from barely being separated to being separated by more than 17 V.

Table 2 summarizes the data for the individual CV spectra shown in Fig. 7. For CV spectra acquired using dried nitrogen, all of the ion CV peak pairs noted showed resolutions higher than one (i.e. baseline resolved) except for the $[M-H]^-$ ion of 2,4 DNT and M^- ion of 2,6 DNT which were overlapping, as noted in Fig. 7a. The maximum resolving power the FAIMS spectrometer achieved with dried nitrogen was ~30. For the CV spectra acquired with ~7000 ppm water vapor added, all of the CV peak pairs showed resolutions well above one and are all baseline resolved. The maximum resolving power the FAIMS spectrometer achieved in these conditions was ~82, due to the increase in CV values while maintaining relatively narrow peak widths.

In general, there were substantial analytical gains made by the addition of solvent vapor to the curtain/carrier gas used for the FAIMS spectrometer. For the three phthalic acid isomers, adding solvent vapor made it possible to fully resolve the ions from one another. Separation of these ions can also be achieved by also increasing the dispersion voltage or by adding carbon dioxide to the carrier gas, but neither approach yields such high resolutions or resolving powers [7,22]. There was a 10× decrease in signal intensity under the solvent vapor conditions used to acquire the CV spectra, but as mentioned above, it is not yet known if the signal decrease is due to FAIMS behavior or ESI behavior. For the explosives analyzed, not only was there a dramatic increase in the separation of the analytes, there was an added benefit of being able to separate individual ionic species for an individual analyte. Signal intensity under the conditions used to acquire the CV spectra were approximately the same as the signal obtained using dried nitrogen only.

4. Conclusions

We have shown the changes in behavior of two different groups of ions with the addition of solvent vapor to the curtain/carrier gas in a high resolving power planar FAIMS spectrometer. The use of a high resolving power enabled us to better monitor position and shape of the CV peaks for individual ions. In general, the ions showed dramatic shifts to larger CV values with the addition of solvent vapor. The shift to larger CV values supports the theory that ions will cluster with solvent and other molecules inside the FAIMS spectrometer at low-fields and then decluster at the high fields of the asymmetric waveform cycle. By monitoring the peak shape and the peak width, it is theorized that different ions may cluster with solvent molecules by different mechanisms. There are substantial analytical benefits provided by adding solvent vapor, although the generality of these results remains to be studied. Further investigations into these observed behaviors may lead to a better understanding of and further development of FAIMS.

Acknowledgement

We would like to acknowledge NSF CBET-0731306 for providing funding for this project.

References

[1] R. Guevremont, R.W. Purves, Electrospray ionization high-field asymmetric waveform ion mobility spectrometry–mass spectrometry, Anal. Chem. 71 (1999) 2346–2357.
[2] R. Guevremont, High-field asymmetric waveform ion mobility spectrometry: a new tool for mass spectrometry, J. Chromatogr. A 1058 (2004) 3–19.
[3] I.A. Buryakov, E.V. Krylov, E.G. Nazarov, E.K. Rasulev, A new method of separation of multi-atomic ions by mobility at atmospheric pressure using a high-frequency amplitude-asymmetric stron electric field, Int. J. Mass Spectrom. Ion Process. 128 (1993) 143–148.
[4] R.W. Purves, R. Guevremont, S. Day, C.W. Pipich, M. Matyjaszczyk, Mass spectrometric characterization of a high-field asymmetric waveform ion mobility spectrometer, Rev. Sci. Instrum. 69 (1998) 4094–4105.
[5] E.A. Mason, E.W. McDaniel, Transport Properties of Ions in Gases, John Wiley & Sons, New York, New York, 1988.
[6] D.A. Barnett, B. Ells, R. Guevremont, R.W. Purves, Separation of leucine and isoleucine by electrospray ionization high-field asymmetric waveform ion mobility spectrometry–mass spectrometry, J. Am. Soc. Mass Spectrom. 10 (1999) 1279–1284.
[7] D.A. Barnett, R.W. Purves, B. Ells, R. Guevremont, Separation of o-, m-, and p-phthalic acids by high-field asymmetric waveform ion mobility spectrometry, J. Mass Spectrom. 35 (2000) 976–980.
[8] L.C. Rorrer III, M. Prieto, R.A. Yost, Evaluation of Linear Injection and Orthogonal Injection into Planr FAIMS-MS, in, Denver, CO, June 1–5, 2008.
[9] E.V. Krylov, Comparision of planar and coaxial field asymmetric ion mobility spectrometer (FAIMS), Int. J. Mass Spectrom. 225 (2003) 39–51.
[10] E.V. Krylov, A method for reducing diffusion losses in a drift spectrometer, Tech. Phys. 44 (1999) 113–116.
[11] R. Guevremont, R.W. Purves, Atmospheric pressure ion focusing in a high-field asymmetric waveform ion mobility spectrometer, Rev. Sci. Instrum. 70 (1999) 1370–1383.
[12] S. Rokushika, H. Hatano, M.A. Baim, H.H. Hill Jr., Resolution measurement for ion mobility spectrometry, Anal. Chem. 57 (1985) 1902–1907.

[13] W.F. Siems, C. Wu, E.E. Tarver, H.H. Hill Jr., P.R. Larsen, D.G. McMinn, Measureing the resolving power of ion mobility spectrometers, Anal. Chem. (1994) 4195–4201.

[14] B.M. Kolakowski, M.A. McCooeye, Z. Mester, Compensation voltage shifting in high-field asymmetric waveform ion mobility spectrometry–mass spectrometry, Rapid Commun. Mass Spectrom. 20 (2006) 3319–3329.

[15] G.A. Eiceman, N. Krylova, E. Krylov, J.A. Stone, Field dependence of mobility for gas phase ions of organophosphorus compounds at atmospheric pressure with differential mobility spectrometry and effects of moisture: insights into a model of positive alpha dependence, Int. J. Ion Mobility Spectrom. 6 (2003) 43–47.

[16] N. Krylova, E.V. Krylov, G.A. Eiceman, Effect of moisture on high field dependence of mobility for gas phase ions at atmospheric pressure: organophosphorus compounds, J. Chem. Phys. 19 (2003) 3648–3654.

[17] G.A. Eiceman, E. Krylov, N. Krylova, E.G. Nazarov, R.A. Miller, Separation of ions from explosives in differential mobility spectrometry by vapor-modified drift gas, Anal. Chem. 76 (2004) 4937–4944.

[18] B.B. Schneider, T.R. Covey, S.L. Coy, E.V. Krylov, E.G. Nazarov, Control of chemical effects in the separation process of a differential mobility mass spectrometer system, Eur. J. Mass Spectrom. 16 (2010) 57–71.

[19] L.C. Rorrer III, R. Guevremont, D.A. Barnett, R.A. Yost, The role of clustering on ion behavior in FAIMS, in: 50th ASMS Conference on Mass Spectrometry and Allied Topics, Orlando, FL, May 31–June 4, 2002.

[20] A.A. Shvartsburg, R.D. Smith, Scaling of the resolving power and and sensitivity for planar FAIMS and mobility-based discrimination in flow- and field-driven analyzers, J. Am. Soc. Mass Spectrom. 18 (2007) 1672–1681.

[21] A.A. Shvartsburg, F. Li, K. Tang, R.D. Smith, High-resolution field asymmetric waveform ion mobility spectrometry using new planar analyzers, Anal. Chem. 78 (2006) 3706–3714.

[22] L.C. Rorrer III, M. Prieto, R.A. Yost, Evaluation of linear injection and orthogonal injection into Planr FAIMS-MS, in: 56th ASMS Conference on Mass Spectrometry and Allied Topics, Denver, CO, June 1–5, 2008.

[23] F.W. Karasek, S.H. Kim, Identification of isomeric phthalic acids by mobility and mass spectra, Anal. Chem. 47 (1975) 1166–1168.

[24] B.M. Kolakowski, Z. Mester, Review of applications of high-field asymmetric waveform ion mobility spectrometry (FAIMS) and differential mobility spectrometry (DMS), Analyst 132 (2007) 842–864.

[25] D. Zhan, J. Rosell, J.B. Fenn, Solvation studies of electrospray ions-method and early results, J. Am. Soc. Mass Spectrom. 9 (1998) 1241–1247.

[26] P. Kebarle, M. Arshadi, J. Scarborough, Hydration of negative ions in the gas phase, J. Chem. Phys. 49 (1968) 817–822.

[27] S. Chowdhury, E.P. Grimsrud, P. Kebarle, Bonding of charge delocalized anions to protic and dipolar aprotic solvent molecules, J. Phys. Chem. 91 (1987) 2551–2556.